Scientific Report

For the project “Novel conjugated polymer structures for high efficiency all-organic solar cells”

Code: PN-II-ID-PCE-2011-3-0274

Phase 2016

Objective 1. Synthesis of photoactive layers from donor oligomers and polymers and acceptors

Task 1.1. Study of photoelectric properties of composite films.

Among oligomers synthesized and characterized previously, four structures (L1, L2, L4 and L5) have been selected to be used together fullerene acceptors in preparation of blends and heterostructures:

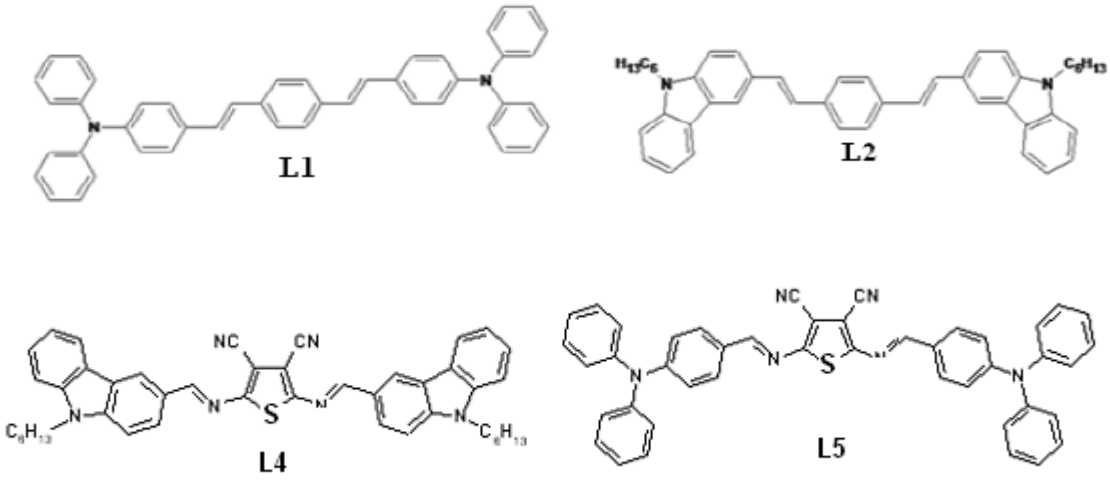

Figure 1. The chemical structure of donor oligomers

As acceptors, two fullerene derivatives have been used: C60 and phenyl C61 methyl ester butyric acid (Figure 2).

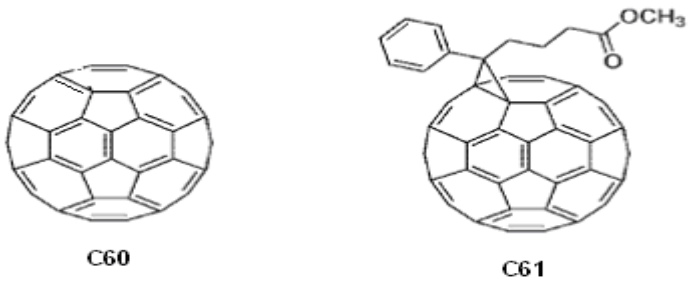

Figure 2. Chemical structure of the fullerene derivatives

A) Linear oligomers, L1 si L2

Thin films of arylenevinylene oligomers have been prepared by vacuum evaporation and deposition on the following substrates: quartz (cleaned with acetone), ITO covered aluminosilicate glass, sheet resistance of 5–15 S.cm (cleaned with acetone) and single crystal silicon wafers (Si) p type with ρ = 2.5 S.cm and n type with ρ = 14 S.cm (cleaned with acetone, hydrofluoric acid and distilled water). The thickness of the thin films deposited by vacuum evaporation evaluated using the ellipsometric method varied between 150 nm and 200 nm. Subsequently, sandwich type semiconductor/insulator/semiconductor (SIS) heterostructures (Fig. 3) have been prepared putting into direct contact the L1 organic layer of the structures Si/L1 and ITO/L1 and, the L2 organic layer of the structures Si/L2 and ITO/L2. Then the sandwiches have been slightly pressed to assure a good contact between the two organic layers (L1/L1 and L2/L2) and the generation of a more uniform intermediate organic layer in the heterostructures Si/L2/ITO and Si/L1/ITO.

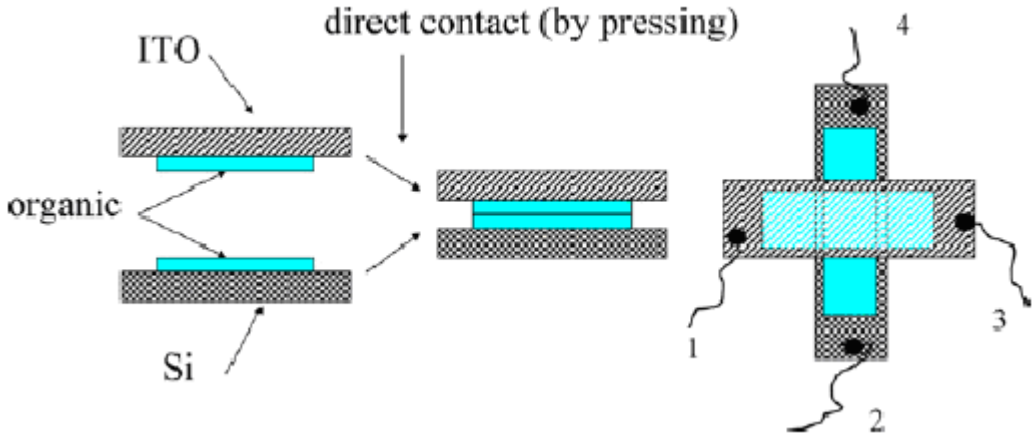

Figure 3: Schematic structures of the oligomer based heterostructures: ITO/oligomer (L1 or L2)/Si (n or p).

A qualitative analysis (shape and position) of the fluorescence spectra of L1 and L2 thin films has revealed for both oligomers, independently of the substrate, a broad structured emission band between 450 nm and 650 nm, with 3 local maxima situated at: 495 nm, 545 nm and 570 nm for L1 (Fig. 4a), and 470 nm, 500 nm and 575 nm for L2 (Fig. 4b). For thin films evaporated on Si and ITO, we have obtained an intense yellow-green fluorescence centred at 545 nm (for L1) and a blue-green fluorescence centred at 575 nm (for L2), while for diluted solution of oligomers in dichloromethane a yellow fluorescence has been evidenced for both oligomers. From the point of view of molecular structure, due to the dihedral angle between the phenyl ring plane and the plane of N-bonded C atoms in triphenylamine oligomer, there exists the tendency to adopt a twisted configuration, which can generate a nonradiative decay by geometrical relaxation and a decrease in the photoluminescence intensity. A similar effect could be obtained by the introduction of carbazole units at terminals of the conjugated backbone, which would result in a less planar molecule. The position of the emission band is the result of the delocalisation of the π-electrons conjugation, through the lone electron pair of the nitrogen atom of the carbazole or triphenylamine end-groups, over the entire conjugated

backbone. The emission peaks of L1 and L2 have shown vibronic structures due to the coupling of the excitation transitions to stretching vibrations.

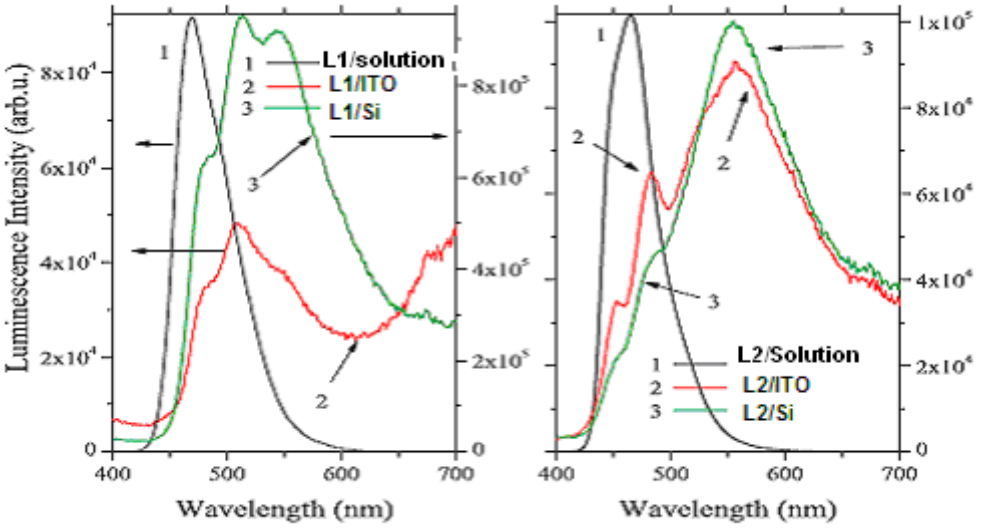

Figure 4. Comparative photoluminescence spectra of L1 and L2 oligomers in dichloromethane and thin films deposited on different substrates (Si, ITO).

The AFM images of the evaporated thin films and the evaluation of the amplitude parameters of the surface have revealed a slightly higher roughness for L2 oligomer (Fig. 5a) [Si (RMS = 15 nm and RA = 9 nm); quartz (RMS = 20 nm and RA = 16 nm); ITO (RMS = 10 nm and RA = 6 nm)] compared to L1 oligomer (Fig. 5b) [Si (RMS = 7 nm and RA = 5 nm); quartz (RMS = 12 nm and RA = 10 nm); ITO (RMS = 3 nm and RA = 2 nm)]. For MAPLE deposited film the higher roughness was obtained for L1 oligomer. This difference is determined by the effect of the solvent on the morphology of the MAPLE deposited films. The SEM images have shown that L1 and L2 films deposited on Si are characterised by compact, small grains morphology (confirmed by the broad XRD peak). Therefore, the optical properties of the prepared oligomeric thin films are explained mainly by the molecular structure and solid state packing of the molecules. We have also shown that these films embedded a lower density of particular structures and aggregates with acicular shape in L1 film (Fig. 5b) and platelet shape in L2 film (Fig. 5a). These low density, randomly distributed structures have been developed during the deposition process.

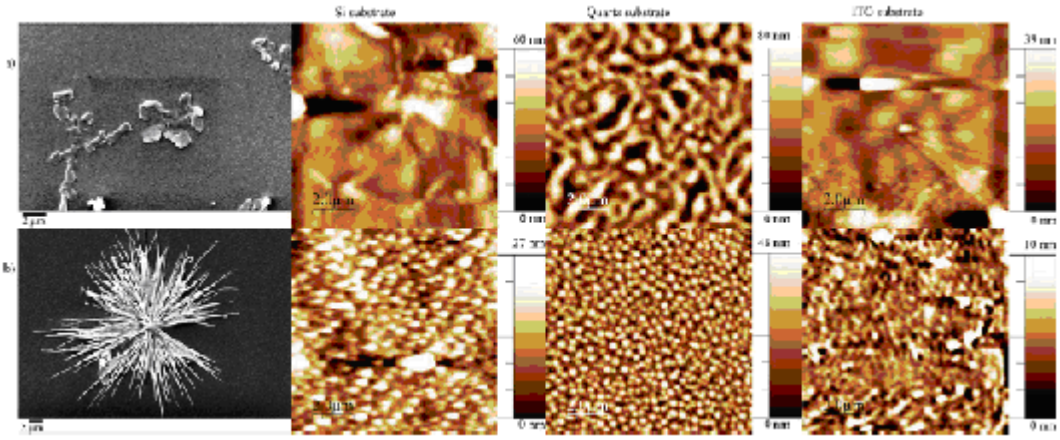

Figure 5: SEM and AFM images of (a) L2 oligomer thin films on Si, quartz and ITO and (b) L1 oligomer thin films on Si, quartz and ITO.

Most of the heterostructures ITO/organic/Si have shown a weak injector contact behaviour both at direct bias and reverse bias (Fig. 6a and b). The limitation of the current by the effect of the space charge was also evidenced by the non-linearity of the log I–log V characteristics. The height of the energetic barriers at the contact ITO/L1 and ITO/L2 are not significantly different, $\delta E_{ITO,L1} = 0.38$ eV; $\delta E_{ITO,L2} = 0.36$ eV and the energy of the conduction band in ITO is $E_{,ITO} = 4.7$ eV, but those at the contacts Si/L1 and Si/L2 eV are different, $\delta E_{Si,L1} = 0.89$; $\delta E_{Si,L2} = 1.15$ eV and the energy of the conduction band in Si is $E_{C,Si} = 4.1$ eV. From these energetic considerations the best conduction was expected in the heterostructure ITO/oligomer/Si realised with L1 intermediate layer. Experimentally, the best injector contact behaviour was obtained in ITO/L1/Si(p) heterostructure (Fig. 6b). Because of the method used to prepare the heterostructures (direct contact) and similar roughness of the L1 and L2 oligomer layers deposited on ITO and Si, this behaviour could be explained by the dominant effect of the organic layer structure. The best conduction was obtained in the heterostructures realised with L1 layer containing acicular clusters

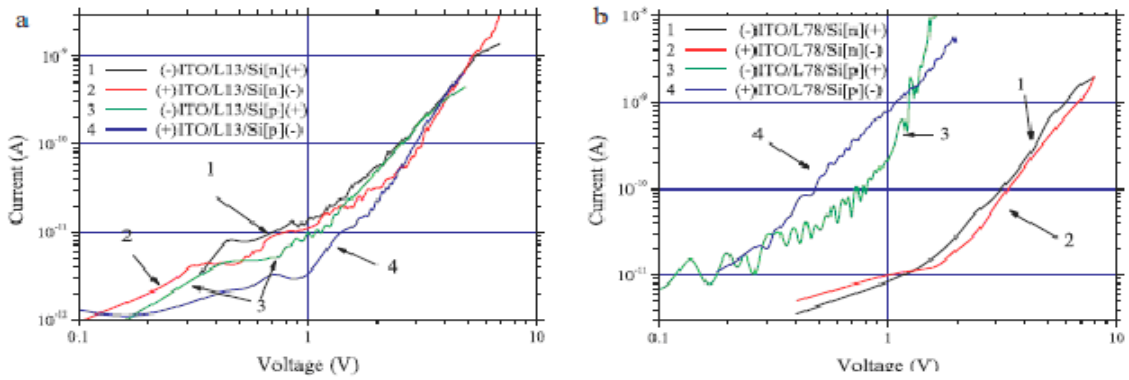

Figure 6. log I–log V characteristics of ITO/oligomer/Si heterostructures at direct bias and reverse bias: (a) oligomer = L13 (L2) and (b) oligomer = L78 (L1).

In conclusion, most of the heterostructures ITO/organic/Si have shown a weak injector contact behaviour both at direct bias and reverse bias. The limitation of the current by the effect of the space charge was also evidenced. The best injector contact behaviour was obtained in heterostructure realised with L1 layer and p-type silicon.

Single and double layer heterostructures have been obtained by MAPLE method from oligomers L1 and L2 as hole transport layer and aluminiu tris(8-hidroxiquinolinat) (Alq3) as electron transport layer. The method has used a laser beam, firstly, the arylenevinylene oligomers were deposited followed by Alq3 layer. The deposition conditions, thickness and roughness of the layers are presented in Table 1.

Table 1

Deposition conditions and RMS/Ra values of the organic heterostructures grown on glass/ITO by MAPLE.

Sample	Substrate	ITO thickness (nm)	ITO resistivity $\times 10^{-4}$ (Ω cm)	No. of pulses	Organic film thickness (nm)	RMS (nm)	Ra (nm)
ITO/1P78	glass/ITO	1620	2.48	80 000	130	35.3	24.6
ITO/2P78	glass/ITO	1580	2.49	160 000	250	36.2	23.8
ITO/1P13	glass/ITO	1200	2.59	80 000	110	10.4	8.2
ITO/2P13	glass/ITO	1230	1.80	160 000	200	12.6	9.0
ITO/1Aq3	glass/ITO	1450	2.70	80 000	160	26.0	18.1
ITO/2Aq3	glass/ITO	1380	2.53	160 000	300	30.1	23.1
ITO/1P78/1Alq3	glass/ITO	–	–	80 000	290	31.8	23.4
ITO/2P78/2Alq3	glass/ITO	–	–	160 000	550	29.1	22.7
ITO/1P13/1Alq3	glass/ITO	–	–	80 000	270	26.2	19.5
ITO/2P13/2Alq3	glass/ITO	–	–	160 000	500	28.5	19.2

Optical properties of the films are studied by FTIR, UV and fotoluminescence. UV–vis spectra revealed that the transparency of the ITO films (Fig. 7a and b) is greater than 80% in the 550–800 nm wavelength range. The contribution of glass substrate was subtracted from all spectra. The thickness of the ITO coatings was calculated from the interference fringes obtained in the UV–vis spectra, considering two successive minima or maxima. Unlike the UV–vis spectra of oligomers MAPLE layers where only the absorption peaks characteristic to the electronic π–π * transition of the conjugated backbone were observed, the UV–vis spectra of oligomers in solution present multiple absorption bands in225–500 nm range. The absorptions in the lower wavelengths range are cut off by the ITO layer deposited on glass substrate. Therefore, in double organic layer heterostructures, the glass/ITOsubstrate hides the absorption peaks which are present in the UV range (Fig. 7(a) and (b)) are characteristic for Alq3. On the other hand, the structure with two organic layers deposited on ITO shows a transparency over 60% for $\lambda > 550$ nm. Alq3 shows important emission properties after the excitationat 350 nm wavelength (Fig. 8(a) and (b)). Depending on the hydroxyquinoline ligands orientation, Alq3 can be found as meridional or facial stereoisomers which are characterized by different optical properties. In our case, the emission bands presented in Fig. 8 were situated around 523 nm and are assigned to the meridional stereoisomer whereas the facial one should appears at shorter wavelength, around 450 nm. The emission band of the L2 oligomer reveals two maxima (490 nm and 525 nm) while in the case of L1 oligomer only one maxim situated at 490–500 nm was visible. The shoulder visible in Fig. 8(a) at small wavelengths is associated to ITO substrate. The emission properties of the heterostructures preserve the shape of the emission band of the Alq3 layer, known for its luminescence.

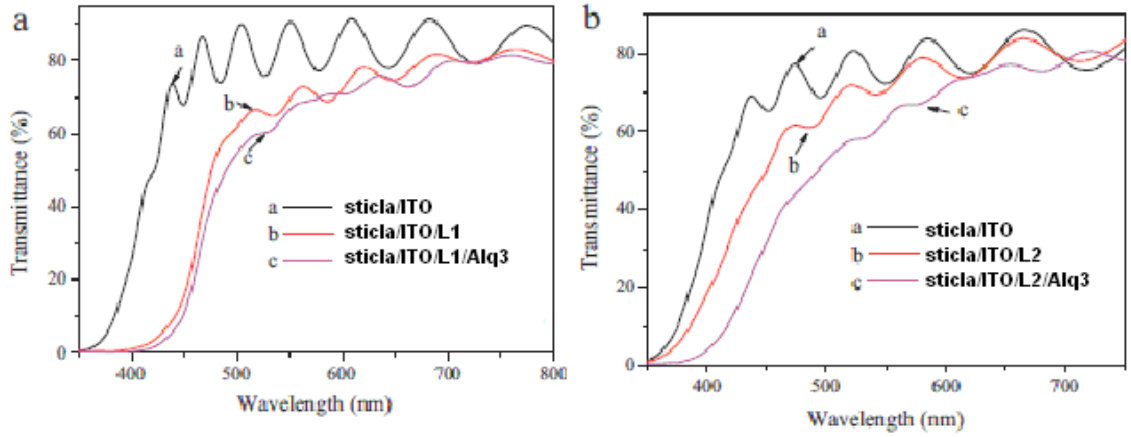

Figure 7. UV–vis spectra of ITO with single and double organic layer structure [(a):ITO/1L1 and ITO/1L1/1Alq3; (b): ITO/1L2 and ITO/1L2/1Alq3].

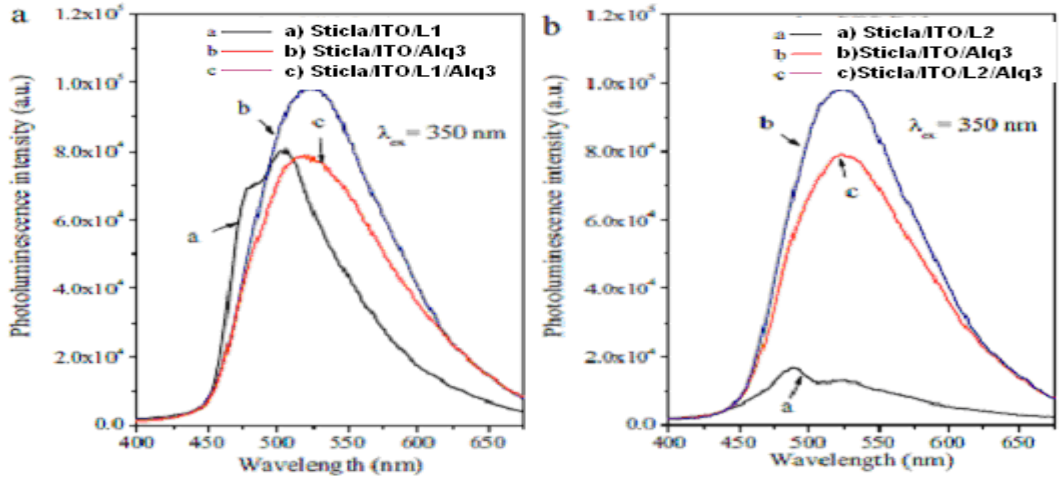

Figure 8. Photoluminescence spectra of single and double layer structures based on (a) 2L1 and (b) 2L2 oligomers.

The morphological features of the films were investigated by atomic force microscopy (AFM) with a MultiView 4000 Nanonics System working in feedback phase with a tip diameter of 10 nm for ITO films and 20 nm for organic films. The investigated area was 2.5 μm × 2.5 μm. ITO layer obtained by PLD was characterized by a low roughness (4.1 nm root mean square (RMS) and 3.1 nm roughness average (Ra)). The MAPLE films were characterized by different morphologies as it can be seen in Fig. 9. L1 film presents a higher roughness compared to L2 film. Thus, the increase of film thickness has not resulted in the increase of the RMS/Ra value(Table 1). Also, the surface morphology has not varied with the film thickness. Unlike the thermal vacuum evaporation process where a higher roughness was observed for L2 layers, the films prepared by MAPLE from L1 oligomer were rougher, in agreement with the previously reported MAPLE depositions. The globular morphology that was mentioned for vacum evaporation films has been also emphasized in these films. From AFM images (Fig. 9) can be remarked a similar morphology and roughness (Table 1) for

Alq3 and L1 films while the roughness of L1/Alq3 heterostructure has slightly decreased. Contrary, in the case of heterostructures based on L2 oligomer, the differences inthe RMS/Ra value of the films lead to a morphology which was typical to the Alq3 film. Considering the particularities of the molecular structure for the L1 and Alq3 compounds, we presumed that the higher roughness has facilitated a better fit. (Fig. 9).

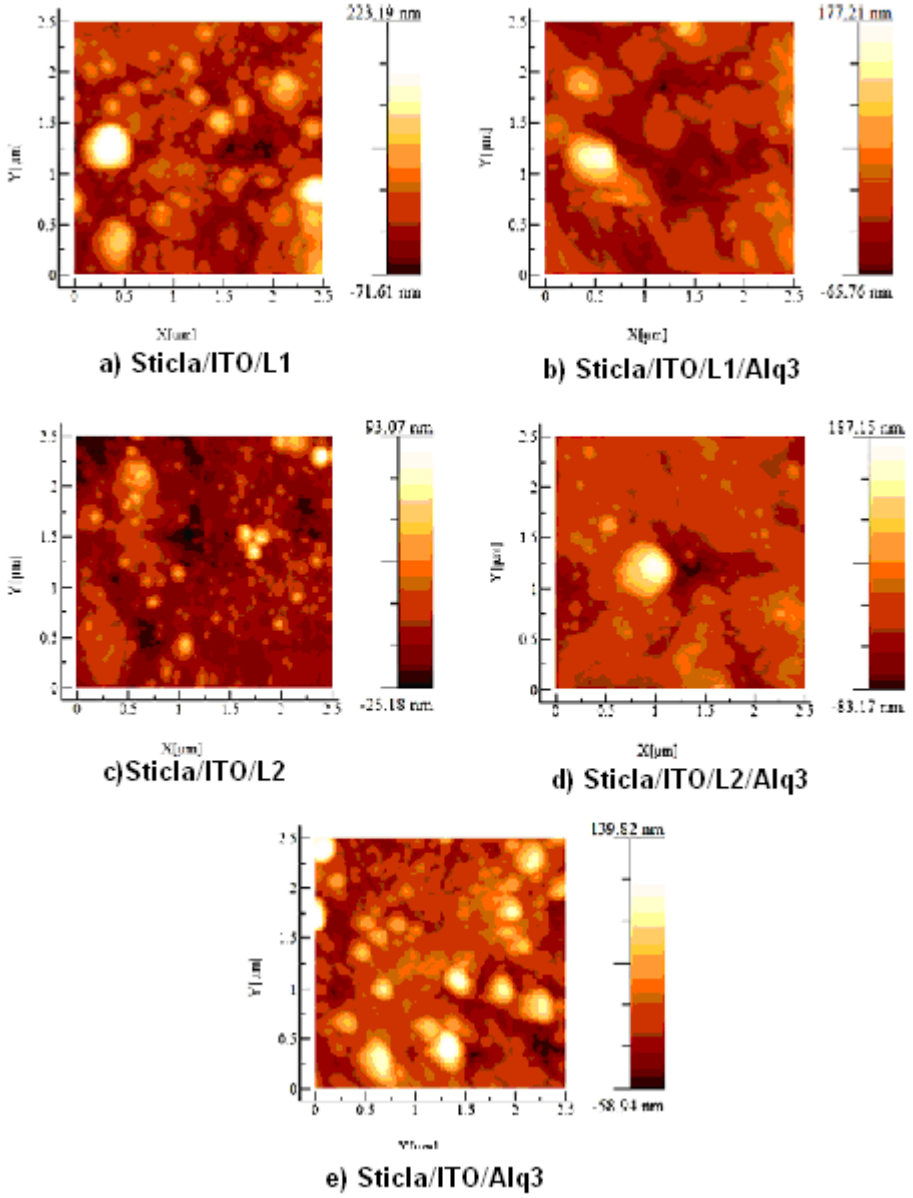

Figure 9. AFM images (a–e) of thin films deposited by MAPLE. Investigated area: 2,5 mμ x2,5 mμ.

In the final step, the electrical properties of the organic heterostructures were investigated. Thus, the values of ITO electrical resistivity were in (1.8×10^{-4} to 2.7×10^{-4}) S. cm range, similar with other previous results obtained for ITO deposited in similar condition. The I–V characteristics of the heterostructures were plot in the 0.1–10 V range in dark conditions (Fig. 10(a)). Generally, the I–V characteristics were symmetrical (Fig. 10(f)) without rectifying properties and behave like injector contacts. The highest value for the current (8×10^{-6}A for 1 V applied voltage) was obtained in thicker bilayer heterostructure based on L1 andAlq3 while the lowest current was determined in

single layer heterostructure based on the thick Alq3 (Table 1). The measured value of the current can not be correlated with the resistivity of the ITO layer because, as it was presented above, there are no significant differences in the calculated values.

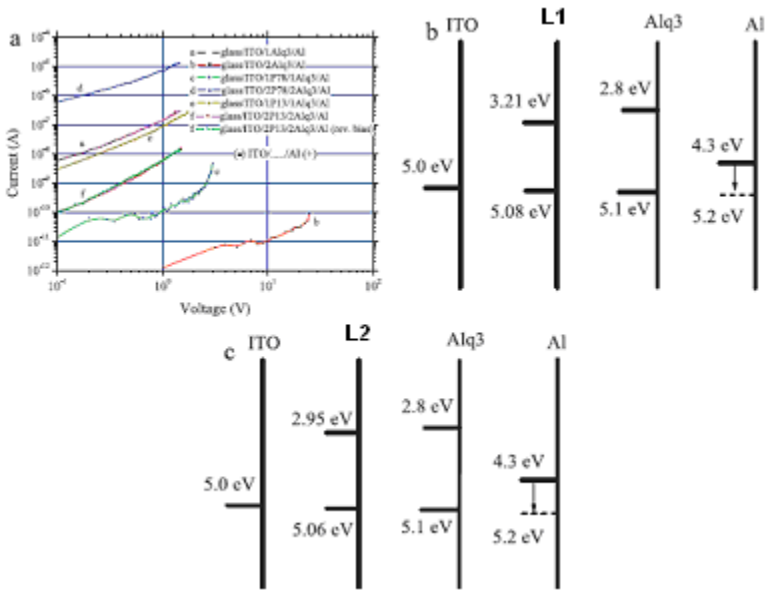

Figure 10. (a) Logarithmic representation of I–V characteristics for ITO/oligomer (L1 or L2)/Alq3/Al and ITO/Alq3/Al heterostructures; (b and c) bands diagrams of investigated heterostructures.

Comparing the Fig heterostructures based on L1 and L2 oligomers it can be seen that the I–V characteristics present opposite behavior. A higher conduction is obtained for the L1 heterostructure with thicker (Table 1) organic layer (ITO/2L1/2Alq3/Al) while, in the case of L2, the best conduction was obtained for the heterostructures with thinner (Table 1) organic layer (ITO/1L2/1Alq3/Al). In both cases, the energetic barrier at the interfaces ITO/organic is very small (Fig. 10(b) for L1 and (c) for L2), because there are no considerable differences in the position of HOMO energetic level of the L2 and L1 oligomer (5.08 eV and 5.06 eV which favors the injection of holes from ITO electrode. Therefore, in these heterostructures with two organic layers are not expected significant differences in the charge carrier flow. The HOMO levels of these two organic layers approximately match with the Fermi level of ITO layer (Fig. 10(b) and (c)). Regarding the Al electrode, at the interface Al/Alq3 is formed a dipole layer characterized by a potential shift of −0.9 V. The effect of this layer is the lowering of the Fermi level of aluminum electrode to −5.2 eV, close to the HOMO level of Alq3.Consequently, all the deposited layers reveal similar positions for the energy levels. Thus, all the interfaces are carrier injectors, and the heterostructure exhibits an ohmic behavior or space charge limited currents for high or low conduction samples. Comparing the structures made only with a single Alq3 layer with those with two layers (L1 or L2 and Alq3) we observed that in the thicker layers (2Alq3; 2L1; 2L2) the current has a noticeable increase (for an applied voltage of 1 V) from 1.5×10^{-12} A in the ITO/2Alq3/Al structure at 7×10^{-9} A and at 8×10^{-6}

A in the ITO/2L2/2Alq3/Al and ITO/2L1/2Alq3/Al, respectively. However, no increase in the conduction of (ITO/1L2 or 1L1/1Alq3/Al) heterostructures based on thin layers was observed. It results that the thickness is a determinant parameter for the electrical conduction in this type of heterostructures and not the energetical and morphological considerations.

Oligomers L1 and L2 were studied also in blend with fullerene C60. The mixed layers oligomer:C60 for a weight ratio between L1 (L2) and C60 of 1:1; 1:2 and 1:3 have been deposited on glass, Si, or glass/ITO substrates maintained at room temperature by matrix-assisted pulsed laser evaporation (MAPLE) using as solvent matrix1,2 dichlorobenzene The effect of the weight ratio between donor and acceptor on the properties of the mixed layers deposited on different substrates (glass, Si and glass covered by ITO) in the same conditions is analyzed with the purpose to select the most adequate donor and the most adequate composition of the mixed layer for potential applications as active layer in photovoltaic applications. The thickness of the mixed organic layers deposited on glass/ITO and of metallic electrode has been evaluated by profilometry with an Ambios Technology XP 100 and it is estimated as the average value of three measurements on each layer (Table 2).

Table 2. Properties of arylenevinylene oligomer:C60 mixed layers deposited by MAPLE on glass/ITO.

Sample	Mixed layer RMS (nm)	Mixed layer RA (nm)	Mixed layer thickness (mμ)	Conductivity of Glass/ITO/Oligomer:C60 (S/cm)
L1:C60 (1:1)	83,8	68,5	5,13	$8{,}41.10^{-13}$
L1:C60 (1:2)	69,1	52,5	2,85	$1{,}22.10^{-12}$
L1:C60 (1:3)	89,3	70,0	4,55	$4{,}12.10^{-12}$
L2:C60 (1:1)	154,0	124,0	4,19	$3.38.10^{-13}$
L2:C60 (1:2)	107,6	82,0	2,70	$3{,}90.10^{-13}$
L2:C60 (1:3)	116,0	92,4	3,96	$7{,}25.10^{-13}$

The optical properties of the mixed layer in the UV–Vis region are determined by the properties of each component: oligomer(L1/L2) and fullerene (C60). The two selected oligomers L1 and L2 films deposited by vacuum evaporation show a large absorption band in UV domain centred on 310–315 nm which is attributed to the n– π* absorption of the triphenylamine moiety in L1 films and to n– π * transition in carbazole aromatic ring in L2 films. This peak preserves in the spectra of L1 films but it is not present in the spectra of L2deposited by MAPLE because the particularities of solid state packing determine weaker polarization interaction between adjacent molecules in the less compact L2 film deposited by MAPLE. The other absorption peak situated between 375 and 475 nm inL1 and L2 is assigned to the π – π* transition of the conjugated electrons along the oligomer backbone chain (Fig. 11). The oligomers band gap indicates that L1 absorbs longer wavelength (until to 660 nm) than L2 (until to 570 nm) and therefore overlaps a larger region of the solar spectrum. Theoretically, the band gap of L1 allows the overlapping with a higher photon flux determining the absorption of more

photons and generation of a higher current which could lead to higher power conversion efficiency. On the other hand, the electronic spectrum of C60 is characterized by several strong UV absorption peaks situated between 200 and 400 nm and a shoulder around 430 nm, which overlap the absorption region in L1 and L2. The low absorption of fullerene in visible range is caused by some forbidden transitions, including the symmetry forbidden transition. Therefore, some modifications appeared in oligomers UV–Vis spectra by blending with fullerene and are associated with intermolecular interactions or generation of new bonds between oligomer and free or clusters of C60, which determine large changes in oligomer's energy levels. Another advantage of L1 andL2 characterized by an Eg around 2 eV is the overlapping of their emission bands with the absorption bands of C60 increasing the photons harvesting.

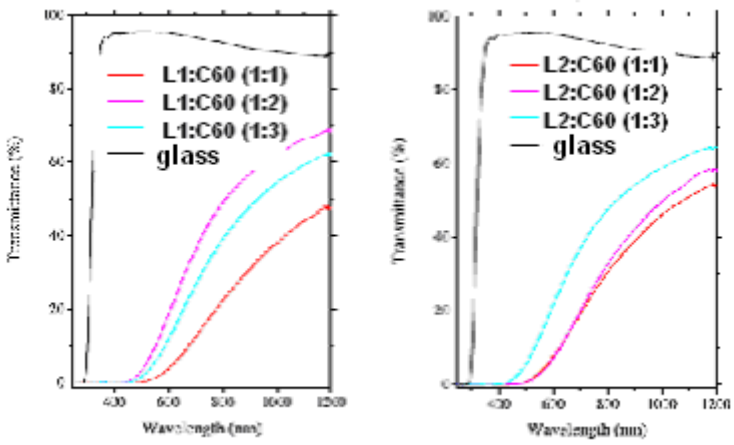

Figure 11. UV–Vis transmission spectra of the of mixed layers oligomer:fullerene in weight ratio 1:1, 1:2, 1:3 deposited by MAPLE on glass substrates: L1:C60(a); L2:C60 (b)

The light scattering process is also sustained by the roughness of the layers evaluated by AFM measurements (Table 2). Independently of the substrate, glass (Fig. 12) and glass/ITO the mixed layer L2:C60 has shown a higher roughness than the mixed layer L2:C60. The surface topography shows hills of different height and valleys suggesting the presence of large or small grains and clusters of grains in both mixed layers. The roughness decreased (RMS L1:C60= 57.9 nm; RA L1:C60= 44.5 nm; RMS L2:C60= 97.8 nm; RA L2:C60= 74.2 nm) when the quantity of fullerene significantly increased (weight ratio = 1:3) both in mixed layer of L1:C60 and L2:C60 deposited on glass (Table 2). For the mixed layer deposited on glass/ITO, the lower roughness (RMS L1:C60= 69.1 nm, RA L1:C60= 52.2 nm; RMS L2:C60= 107.6 nm, RA L2:C60= 82.0 nm) has been obtained at a weight ratio between L1 (L2) and fullerene of 1:2 (Table 2). A lower roughness assures a better contact between the organic layer and the Al electrode and a more efficient charge carriers' collection. For both mixed layers, L1:C60 and L2:C60, a better charge carrier collection is anticipated for a weight ratio between oligomer and C60of 1:2. During the MAPLE deposition under the effect of laser radiation appear droplets and clusters of droplets having different size and

containing molecules of polymer, fullerene and solvent matrix. This mechanism is a consequence of the explosive decomposition under the effect of the laser beam determined by the overheating of a region of the target surface surpassing the limits of the thermodynamic stability. When arrive at the substrate surface the clusters decompose in liquid droplets forming the film and gaseous matrix molecules which are removed by pumping from the deposition chamber. The droplets which deposit on the substrate held at room temperature determine a characteristic structure of oligomer:C60 film showing special types of local organization which are randomly distributed, like grains/granules or/and large-scale structures, clusters of grains. These structures dispersed in a compact layer can have different dimensions and different shapes, including spherical ones, and contain only one component (polymer or fullerene) or both components (polymer and fullerene). The presence of grains is confirmed by the AFM measurements. The morphology depends on the droplets evaporation mechanism because the solvent can evaporate partially or totally. Sometimes a fraction of the matrix molecules can be retained inside the droplets and their evaporation is prevented by the polymer and fullerene molecules which are pushed to the periphery of the droplet under the effect of the matrix vapour. The morphology of the layers showing granular structures with irregular shape (Fig. 12b, c, e and f) can appear under the effect of the inside matrix molecules vapor pressure causing the droplet expanding and breaking. Especially for high weight ratio between oligomer and C60 (1:2 and 1:3), the layers ofL2:C60 (Fig. 12e and f) show some larger grains or clusters of grains generated during the deposition than the layers of L1:C60 (Fig. 12 b and c). The luminescence of the mixed layers deposited on glass (Fig. 13) depends on the luminescence properties of each component: oligomer (L1, L2) and C60 at λ excitation= 335 nm (Fig. 13 a and c) and λ excitation= 435 nm (Fig. 13 b and d). The luminescence of fullerene is very low because of the symmetry forbidden transition HOMO–LUMO, S1→ S0, and of the efficient non radiative transition by intersystem crossing mechanism. This decay between states of different multiplicity from singlet (S1) on triplet (T1) is characterized by high yield and could be followed by a radiative deexcitation by phosphorescence emission from the triplet excited state (T1) toS0. The PL spectrum of L1 (L2): C60 (Fig. 13) is determined by the radiative transition between the five fold-degenerated HOMO orbital and three fold-degenerated LUMO orbital in C60. Thus the PL band with a peak situated between 450 nm and 550 nm for λ excitation= 335 nm and, between 480 nm and 580 nm for λ excitation= 435 nm in oligomer:C60 blends can be the result of the relaxation of the forbidden transition from HOMO to LUMO which is characteristic for C60. The relaxation of the selection rules is a consequence of the interaction between each molecule and the surrounding molecules in the solid state determining the lowering of the molecule symmetry, removing the degeneracy and allowing new transitions. Polarization interactions of molecules with surrounding medium are due to the high polarizabilities of the π-conjugated chain. The PL peak situated between 680–745 nm in the emission spectra of the mixed layers at λ excitation= 435 nm (Fig. 13 b and d) can also be attributed

to C60 and it is situated bellow the forbidden HOMO–LUMO transition. We have to consider also the contribution of the substrate situated around 430 nm for λ excitation= 335 nm and around 530 nm for λ excitation= 435 nm. Beside C60, the emission behaviour of oligomers as components of the mixed layer is also very important, their emission bands being situated between 400 nm and 600 nm and overlapping the emission band of fullerene. The delocalisation of the π electrons over the entire conjugated backbone involving the lone electrons of the N atoms, determines the position of the emission bands. Because of the dihedral angle between the phenyl ring and N C bond planes in triphenylamine oligomer (L1) it is favoured a twisted configuration which generates the nonradiative decay by geometrical relaxation through intersystem crossing. The deviation from planarity is also generated by introducing carbazole units at the terminals of conjugated chain (L2) and determines a nonradiative decay. In both cases this non-radiative decay can reduce the intensity of the PL emission of the mixed layers. Because both L1:C60 and L2:C60 show a substantial matching between the spectral range of sensitivity and the photoluminescence region necessary in photovoltaic applications, both oligomers are appropriate for using as donor in mixed active layer in solar cell structures. Considering glass/ITO as transparent conductor electrode for building the solar cell structure the emission peaks of this substrate fit very well the emission peaks of the mixed layers both at excitation with λ = 335 nm and λ = 435 nm and therefore ITO film does not affect the PL properties of the L1 (L2): C60 mixed layers.

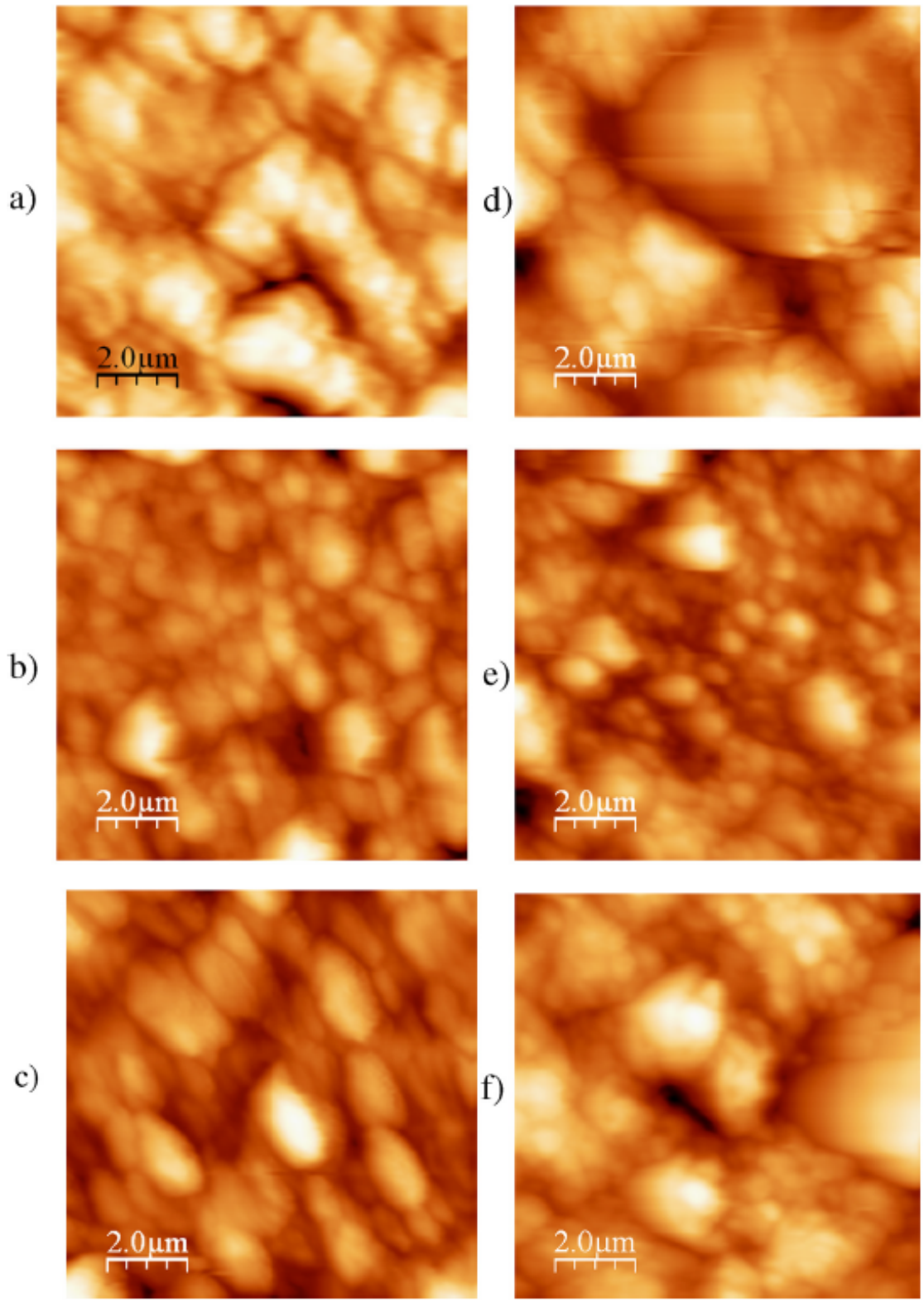

Figure 12. AFM images of oligomer:fullerene mixed layers deposited by MAPLE on glass substrates: L1:C601:1 (a); L1:C601:2 (b); L1:C601:3 (c); L2:C601:1 (d); L2:C601:2(e); L2:C601:3 (f).

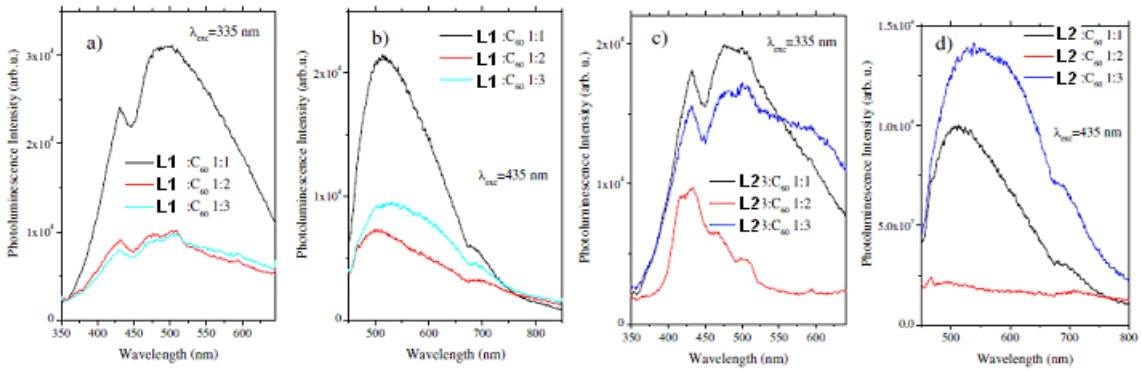

Figure 13. Photoluminescence spectra of mixed layers of oligomer:fullerene in weight ratio 1:1, 1:2, 1:3 deposited by MAPLE on glass: L1:C60, λexc. = 335 nm (a); L1:C60, λexc.= 435 nm (b); L2:C60, λexc.= 335 nm (c); L2:C60, λexc.= 435 nm (d).

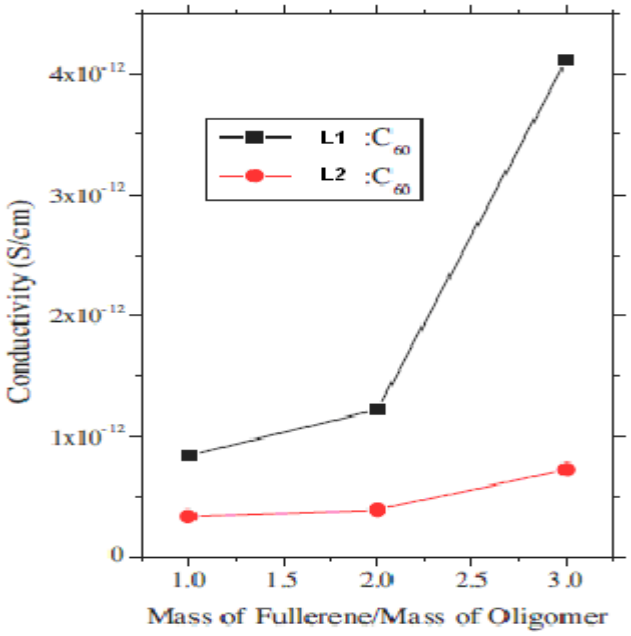

Figure 14. Dependence of the oligomer:fullerene, L1(L2):C60, mixed layers conductivity by layer composition.

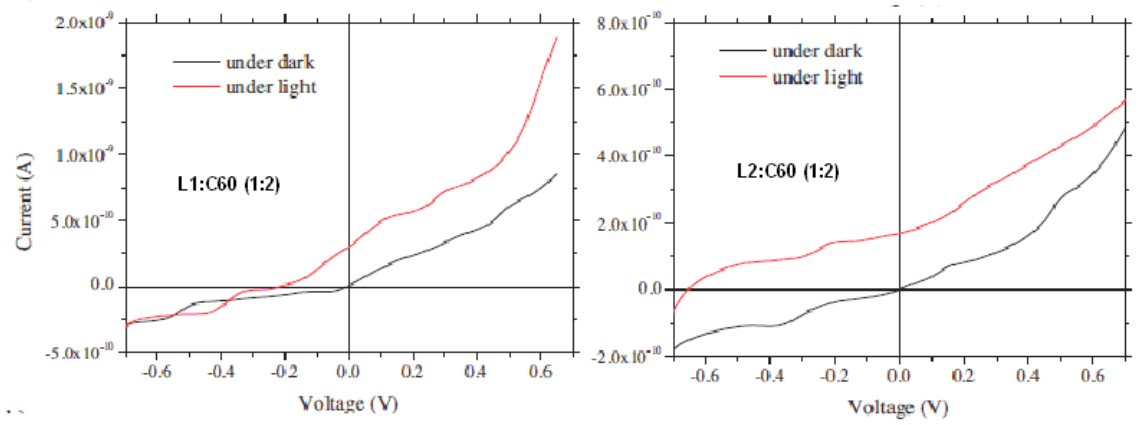

Figure 15. I–V characteristics for structures with oligomer:fullerene (1:2) mixed layer:glass/ITO/L1:C60/Al (a); glass/ITO/L2:C60/Al (b).

The conductivity (Table 2) of the structures realized with L1 was higher than the conductivity of the structures realized with L2 and an increase in the conductivity of the mixed layer can be obtained increasing the fullerene concentration (Fig. 14). The structures glass/ITO/oligomer:C60 (weight ratio 1:2)/Al have shown slightly asymmetric non-linear I–V characteristics in dark (Fig.16). The dark current is small, 10^{-9} A (at 0.7 V) in the structure realized with L1:C60 mixed layer (Fig. 16a) and $\sim 5 \times 10^{-10}$A (at 0.7 V) in the structure realized with L2:C60 mixed layer (Fig. 16b).We have also evidenced a photovoltaic effect in the structures realized on glass using ITO and Al electrodes and mixed layers ofL1:C60 and L2:C60 in weight ratio 1:2. These are the L1:C60 and L2:C60 layers characterized by the lowest surface roughness which theoretically favours the charge carriers collection by the Al electrode and the lowest Urbach energy associated with a reduced loss of carriers by scattering/recombination on disorders/defects. At illumination, the highest current (1.5×10^{-9} A at 0.6 V) has been obtained in sample containing a L1:C60 (1:2) mixed layer. These low values obtained for the current are determined mainly by two factors affecting the charge carrier transfer from oligomer to C60: the morphology of the mixed layer characterized by the presence of large fullerene crystalline clusters which affect the charge transfer from donor to acceptor and the thickness of the layer which favours the loss of charge carriers by recombination on defects associated with disorder, reducing the number of the carriers collected by electrodes. From energetic point of view, considering the position of HOMO and LUMO levels in oligomers determined by cyclic voltammetry and the work function of ITO (4.7 eV) and Al (4.3 eV), the energetic barriers at the contact between the mixed layer and electrodes give a more favourable global energetic balance for the solar cell structures realized with oligomer L1 than L2 and therefore the current is slightly higher in L1:C60. Analyzing the solar cell structures glass/ITO/L1:C60/Al and glass/ITO/L2:C60/Al, the best values of the open circuit voltage and fill factor parameters, Voc= 0.66 V and FF = 0.37 (Table 3) have been obtained in the structure with a mixed layer prepared by MAPLE from L2:C60 (1:2) blend. This confirms that in the case of the selected oligomers, the parameters of the solar cell structures are determined not by the energetic balance and surface topography but by other factors correlated with the internal morphology at the nanometer scale which probably is more favourable in the case of L2:C60. For each oligomer:fullerene mixed layer the thickness has an optimum as a compromise between the necessity to assure the absorption of a higher number of incident photons to generate an increased number of excitons, requiring thick layers and necessity to avoid the recombination of generated excitons before dissociation in free charge carriers, requiring thin layer. Considering the short diffusion length of excitons, thick layers are not favourable for generation of charge carriers to be subsequently collected by electrodes. Therefore the possibility to increase the performance of the solar cell structure with L1:C60 and L2:C60 active layers increases by reducing the thickness of the active layer. The mixed layers deposited on glass/ITO with a weight ratio

between the two components of (1:2) are characterized by the lowest thickness and the lowest roughness assuring a good contact with the collecting electrode. For the other two mixtures (1:1) and (1:3) even in principle the decreasing in thickness could increase the parameters of the solar cells, the higher roughness of the layer surface obstructs the collection of the charge carriers. The thickness of the mixed layer depends on the behaviour of the added fullerene and its incorporation in the layer which is difficult to predict: it can remain dispersed or form clusters depending on the quantity and solubility in the selected solvent. For a weight ratio between oligomer and fullerene of 1:2 it seems to be obtained small fullerene clusters showing low differences hill-valley and assuring low roughness and thickness of the layers.

In conclusion, the photovoltaic effect has also been evidenced in the structures realized with L1:C60 and L2:C60 weight ratio 1:2 mixed layer sandwiched between ITO and Al electrodes. These are the L1:C60 and L2:C60 layers characterized by the lowest surface roughness favouring the charge carriers collection by the Al electrode and lowest Urbach energy associated with a reduced loss of carriers by scattering on disorders. The solar cell structure realized with a L2 : C60 (1:2) mixed layer has shown the best Voc (0.66 V) and FF (0.37) parameters. Therefore, the MAPLE prepared L2:C60 weight ratio 1:2 mixed layer is a promising active medium for solar cells applications.

Table 3. Parameters of the solar cells structures realized with arylenevinylene oligomer: C60 mixed layers.

Proba	Pmax (V). 10^{11}	Voc (V)	Isc (A).10^{10}	FF
L1:C60 (1:2)	1,5	0,23	2,9	0,22
L2:C60 (1:2)	4,2	0,66	1,7	0,37

Oligomers having donor and acceptor groups (L4 and L5).

Mixed heterostructures L4/L5: C61

The mixed layers oligomer L4 (L5)/fullerene C61 have been deposited by a laser technique (MAPLE) on glass/ITO substrates with area of 25 mm x 25 mm using chloroform or DMSO as solvents for matrix. The laser beam is characterised by energy of 100 mJ and a spot area of 32 mm^2 assuring a fluence of 312 mJ/cm^2.

Both single L4 and L5 layers show a large absorption band between 350 nm and 650 nm. The mixed layers show a very good transmission (>70 %) over 600 nm and a degree of scattering confirmed by the slope of the absorption edge (Figure 16). The comparative FTIR spectra (Figure 17) of MAPLE and drop cast deposited mixed films on Si have confirmed the preservation of the chemical structure during the laser deposition. This means that MAPLE is an adequate method for the preparation of oligomer:fullerene derivative mixed layers.

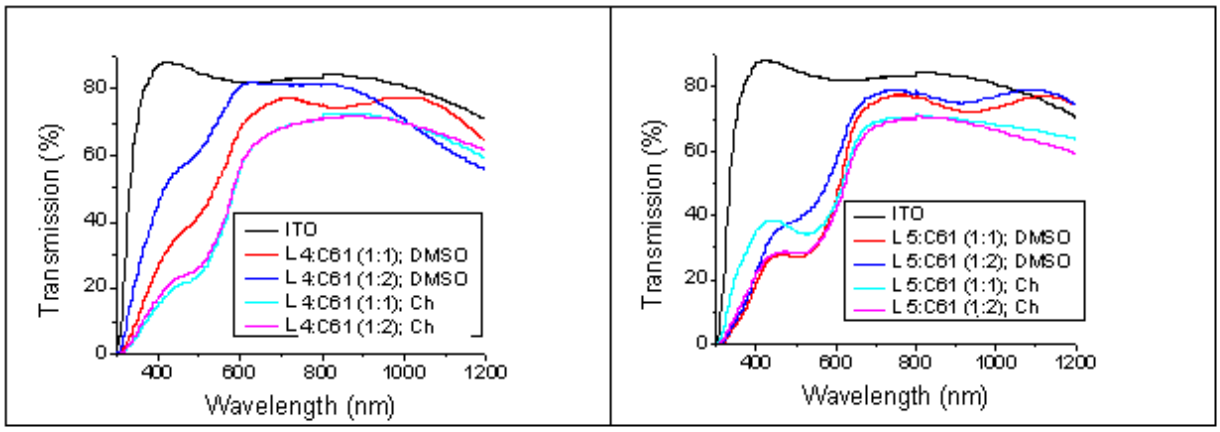

Figure 16. UV-vis spectra of L4/C61 and L5/C61

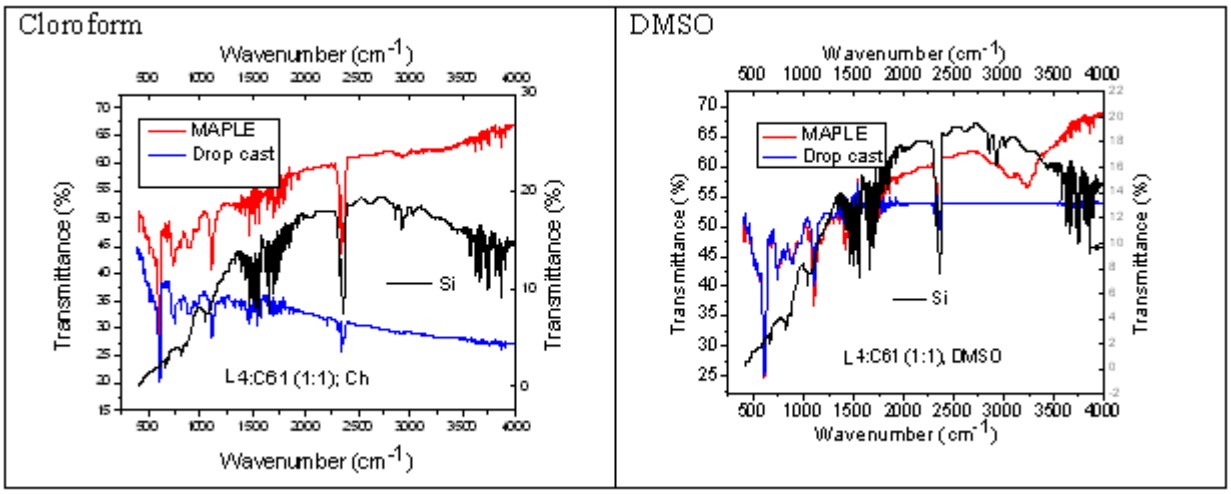

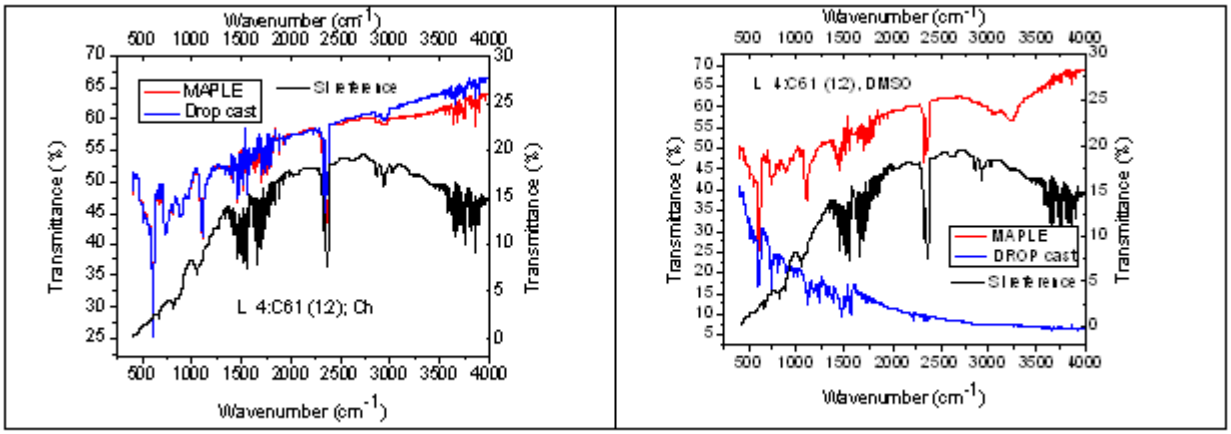

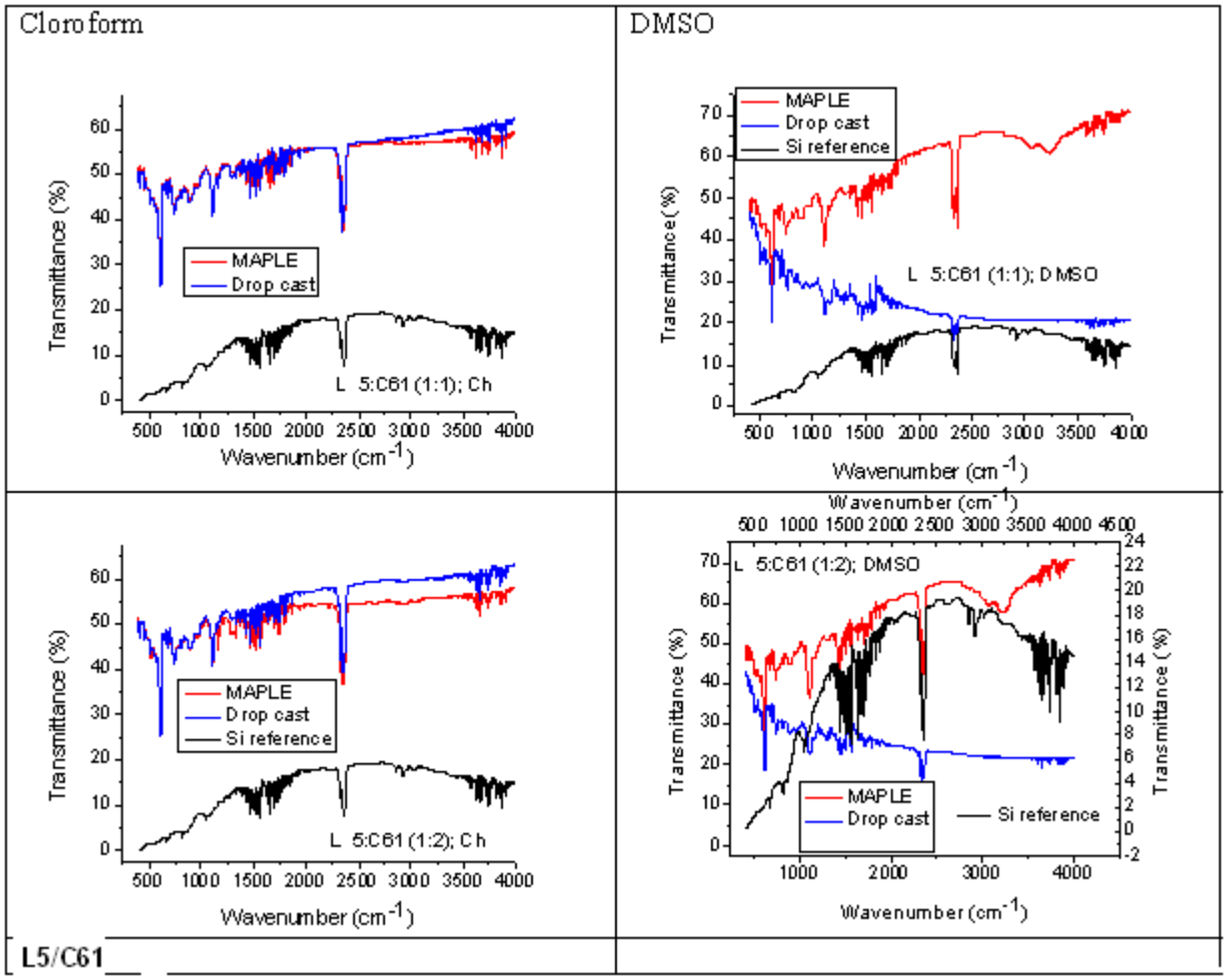

Figure 17. FTIR spectra of the mixed layers of oligomer: fullerene C61 in weight ratio 1:1 and 1:2 deposited by MAPLE and drop cast on Si.

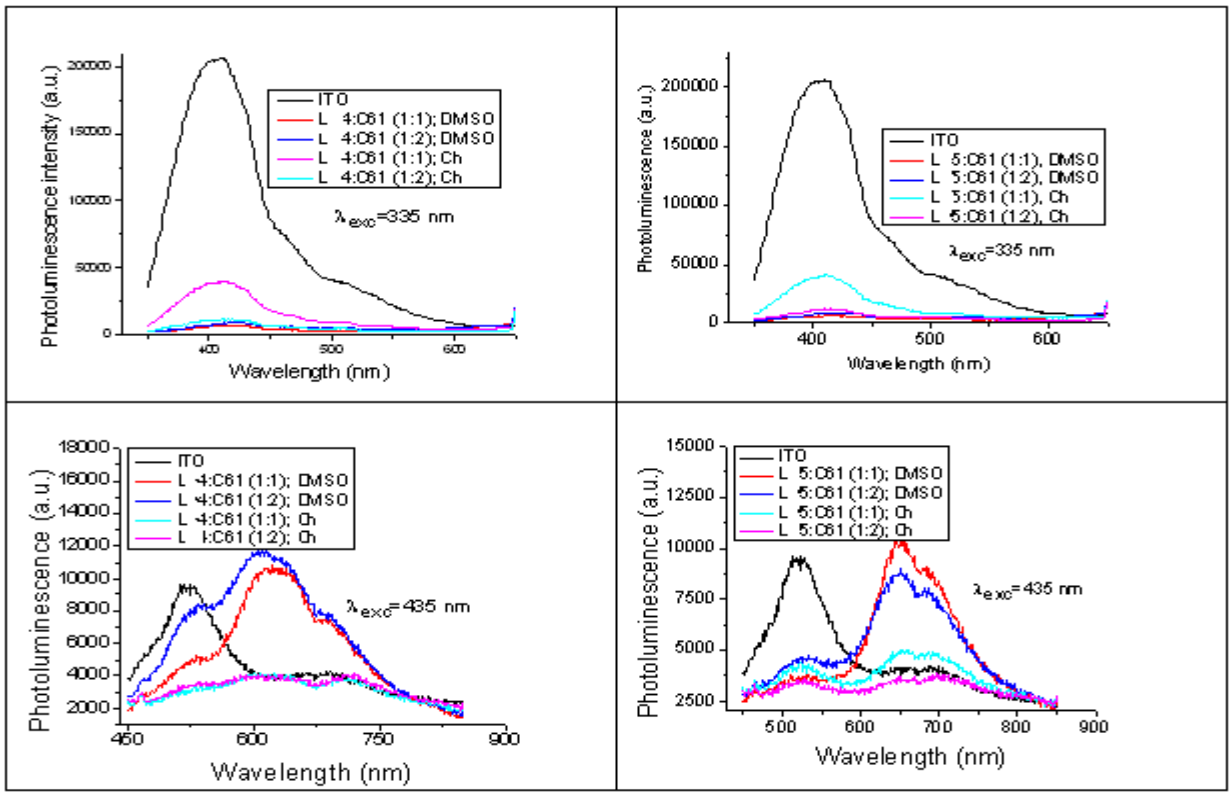

Figure 18. Photoluminescence spectra of mixed layers of oligomers / fullerene C61 in weight ratio 1:1 and 1:2 deposited by MAPLE on ITO

The photoluminescence (PL) spectra (Figure 18) of the mixed layers at excitation with λ=335 nm is dominated by the strong emission of the ITO film deposited on glass with a peak at ~410-415 nm. This radiation situated around 410 nm is strongly attenuated in the mixed layers independent of the used solvent, because the wavelength is situated in the absorption range of the mixed layer. At excitation with wavelength situated in visible domain, λ=435 nm, the layers obtained using DMSO as matrix show a stronger emission intensity compared to the layers obtained using chloroform as matrix characterized by an emission peak at ~650 nm with a shoulder at 720 nm situated in the transmission domain of the mixed layer independent of solvent. This behavior can be determined by the particularity of the oligomer layer formation, the assembling in a layer of the oligomer molecules evaporated from the target containing DMSO being different from that of the molecules evaporated from the target containing cloroform.

Layer morphology

AFM and SEM images (Figure 19 and 20) have revealed for the layers deposited from DMSO grain-like clusters (aggregates) of different dimensions dispersed in a relatively smooth film. For a given weight ratio (1:1 or 1:2), the layers obtained both with oligomer LV4 and LV5 deposited from DMSO are characterized by a lower roughness than the same layers deposited from chloroform (Table 4). Also, an increase in the roughness has been also observed with the increase in fullerene derivative concentration, weight ratio oligomer:fullerene increase from 1:1 to 1:2 (Table 4).

L4:C61 (1:2) Ch, ITO **RMS=60,2 nm; RA=46,8 nm**

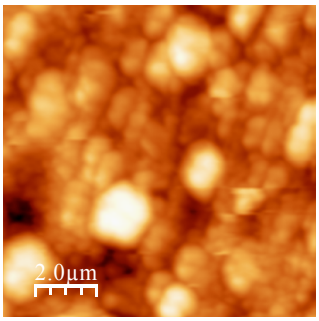

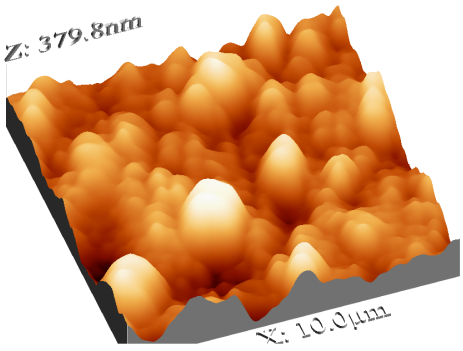

L4:C61 (1:2) DMSO, ITO **RMS=30,2 nm; RA=23,9 nm**

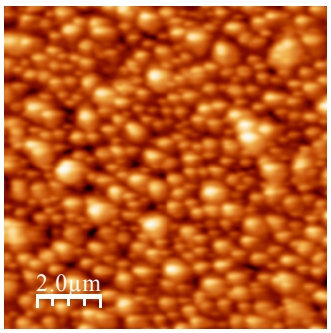

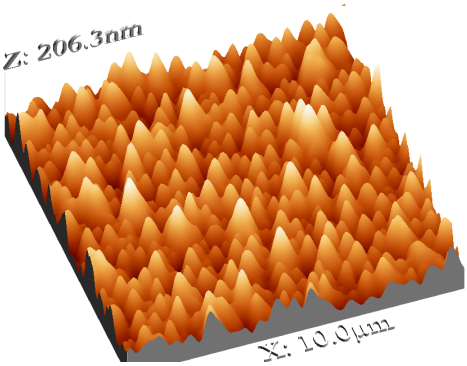

L5:C61 (1:2) Ch, ITO **RMS=45,1 nm; RA=35,1 nm**

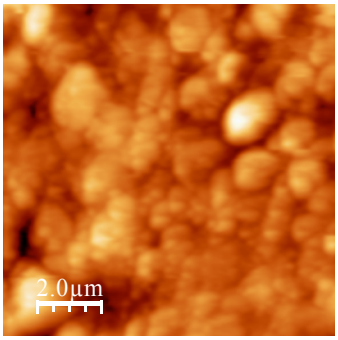

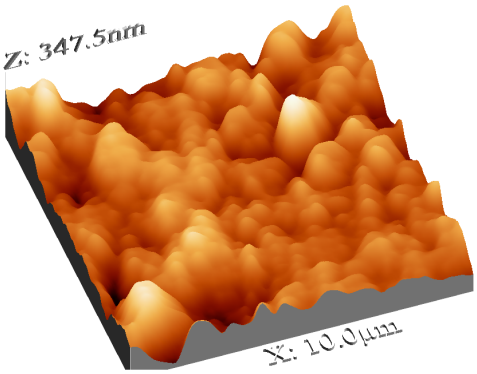

L5:C61 (1:2) DMSO , ITO **RMS=59,9 nm, RA=41,0 nm**

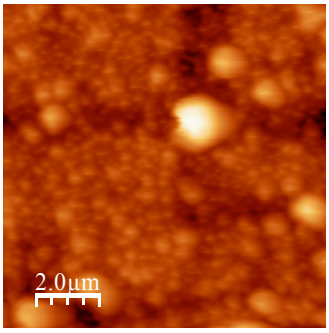

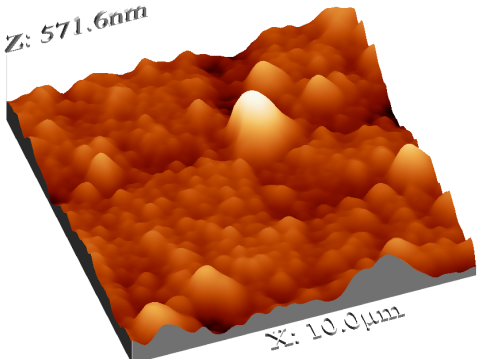

Figure 19. AFM images of L4/C61 and L5/C61 at two weight ratios deposited on ITO substrates.

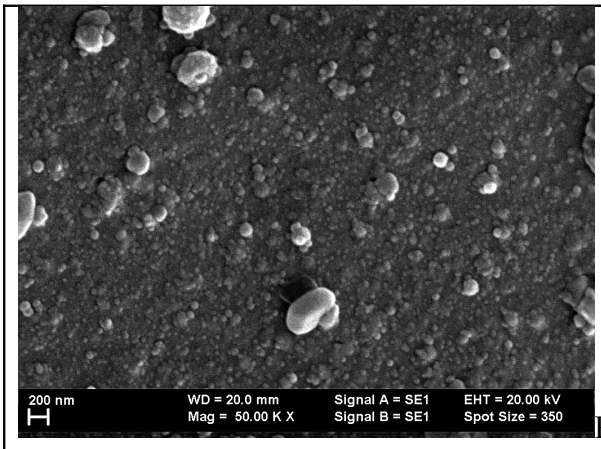

Pr1

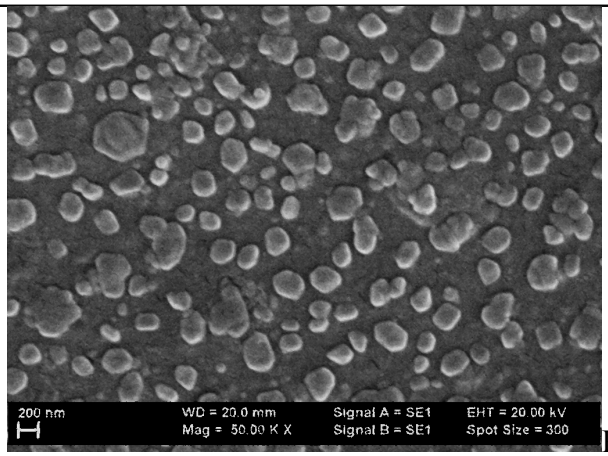

Pr2

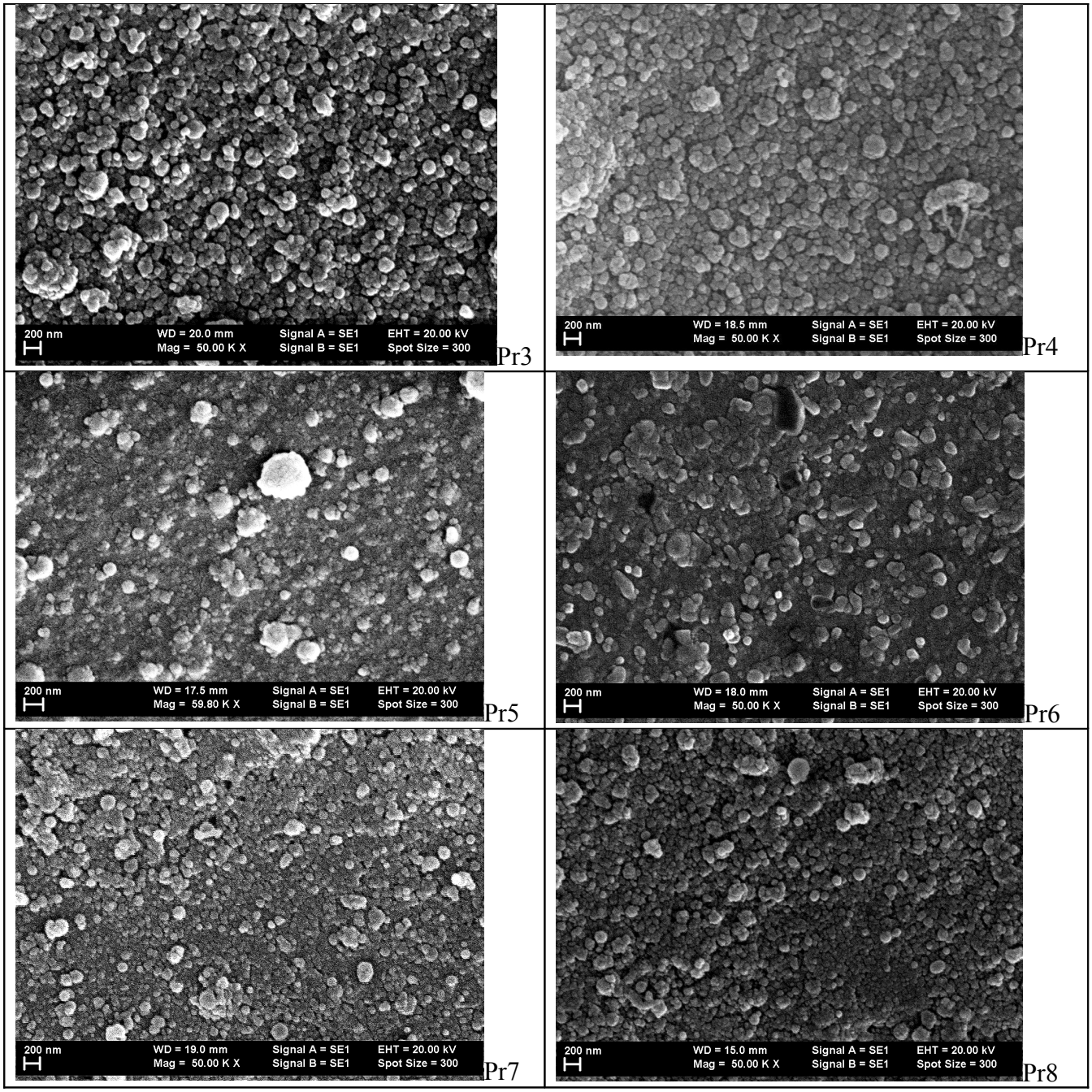

Figure 20. SEM images of oligomer L4/C61 and L5/C61 mixed layers deposited by MAPLE on glass or ITO substrates: L4:C61 (1:1) Ch, Glass (Pr1); L4:C61 (1:1) DMSO (Pr 2), glass L4:C61 (1:2) Ch, ITO (Pr 3) L4:C61 (1:2) DMSO, ITO (Pr4); L5:C61 (1:1) Ch, glass (Pr5) L5:C61 (1:1) DMSO (Pr 6), glass; L5:C61 (1:2) Ch, ITO (Pr 7) L5:C61 (1:2) DMSO, ITO (Pr8)

SEM images show for sample prepared from DMSO grains of different dimensions containing only one component, oligomer or fullerene, or both components oligomer and fullerene and sometimes the captive DMSO (Pr1, Pr2, Pr5, Pr6). For layers deposited using chloroform as matrix a more uniform morphology resulted from the compact stacking of smaller dimension grains of mostly spherical shape, very well defined was observed (Pr3, Pr4, Pr7, Pr8).

Photovoltaic properties

The electrode Al was deposited by vacuum evaporation.

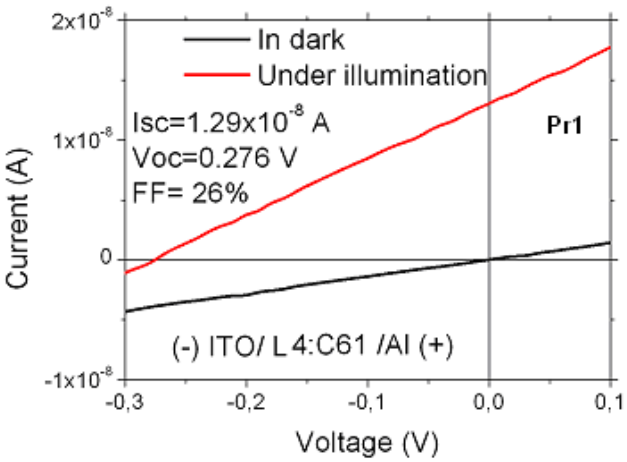

Pr1=L4:C61 (1:1), Ch

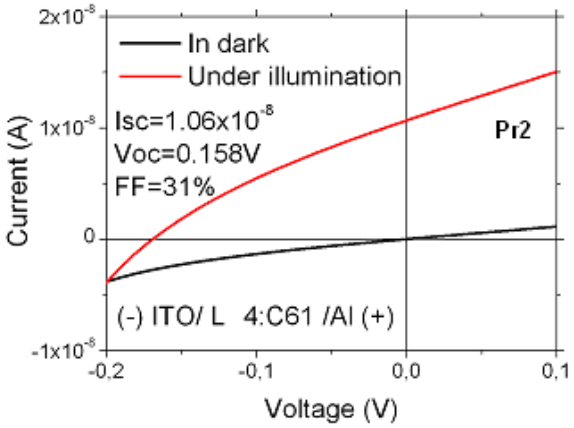

Pr2=LV:C61 (1:2), Ch

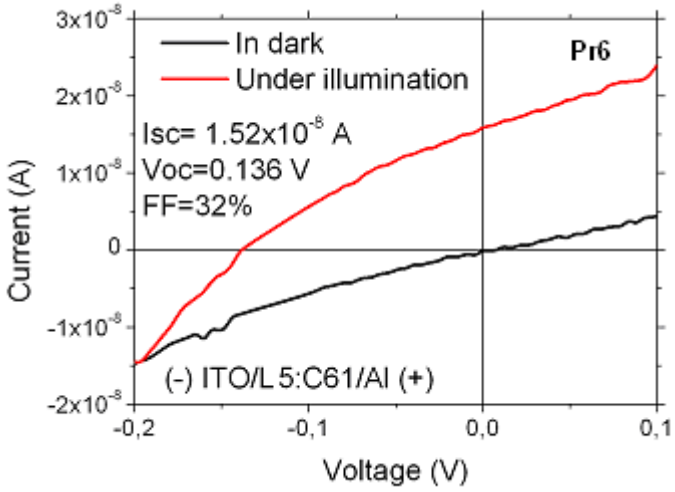

Pr6=L5:C61 (1:2), Ch

Figure 21: I-V characteristics for heterostructures L4(L5)/C61

The mixed layers L4(L5)/C61 (1:2 mass ratio) show photovoltaic properties (Figure 21).

A photovoltaic effect is obtained in the heterostructures with mixed layer deposited from chloroform characterized by a roughness favoring a bigger contact surface between active layer and electrode and a better collection of the charge carriers. The energetic considerations sustain a more significant photovoltaic effect in the heterostructure realized with L5 from chloroform matrix compared to photovoltaic effect in heterostructure realized with L4 from chloroform matrix. The highest dark

current around $2.5x10^{-6}$ A for an applied voltage of 0.1 V is shown by the heterostructure glass/ITO/ L5:C61 (1:1) prepared from a chloroform matrix. The increase in V_{OC} for the heterostructure obtained with L4 is correlated with the lower position of HOMO level in L4. In our solar cell structures FF is mostly determined by the roughness of the mixed layer but a limitation can be introduced by space charge accumulation effect and recombination on defects generated during MAPLE deposition (Table 5).

Table 4: Organic oligoazomethine: fullerene derivative mixed layer deposited by MAPLE from chloroform and DMSO matrix: roughness and thickness

Sample	Active layer RMS (nm)	Active layer RA (nm)	Active layer thickness (nm)
L4:C61 (1:1), Ch-Pr1	44.2	34.7	240
L4:C61 (1:2), Ch-Pr2	60.2	46.8	275
L4:C61 (1:1), DMSO-Pr3	27.6	19.9	365
L4:C61 (1:2), DMSO-Pr4	30,2	23.9	260
L5:C61 (1:1), Ch-Pr5	50.6	37.8	210
L5:C61 (1:2), Ch-Pr6	61.3	45.2	205
L5:C61 (1:1), DMSO-Pr7	23.5	16.6	230
L5:C61 (1:2), DMSO-Pr8	59.9	41.0	260

Table 5: Parameters of the solar cell structures realized with oligoazomethine oligomers: C61 mixed layers.

Sample	V_{OC} (V)	I_{SC} (A)	FF (%)
LV4:C61 (1:1), Ch-Pr1	0.32	$1.3x10^{-8}$	25
LV4:C61 (1:2), Ch-Pr2	0.18	$1.1x10^{-8}$	29
LV5:C61 (1:1), Ch-Pr5	0.30	$4.0x10^{-8}$	35
LV5:C61 (1:2), Ch-Pr6	0.12	$1.7\ x10^{-8}$	30